

Posterior cingulate cortex atrophy and regional cingulum disruption in mild cognitive impairment and Alzheimer's disease

IL Han Choo^a, Dong Young Lee^{a,b,*}, Jongsu S. Oh^c, Jae Sung Lee^c, Dong Soo Lee^{b,c},
In Chan Song^d, Jong Choul Youn^e, Shin Gyeom Kim^a, Ki Woong Kim^f,
Jin Hyeong Jhoo^g, Jong Inn Woo^{a,b,h}

^a Department of Neuropsychiatry and Clinical Research Institute, Seoul National University Hospital, Seoul, Republic of Korea

^b Interdisciplinary Program for Cognitive Science, Seoul National University, Seoul, Republic of Korea

^c Department of Nuclear Medicine, Seoul National University Hospital, Seoul, Republic of Korea

^d Department of Radiology, Seoul National University Hospital, Seoul, Republic of Korea

^e Department of Neuropsychiatry, Kyunggi Provincial Hospital for the Elderly, Yongin, Kyunggi, Republic of Korea

^f Department of Neuropsychiatry, Seoul National University Bundang Hospital, Seongnam, Kyunggi, Republic of Korea

^g Department of Psychiatry, Kangwon National University Hospital, Chuncheon, Kangwon, Republic of Korea

^h Neuroscience Research Institute of the Medical Research Center, Seoul National University, Seoul, Republic of Korea

Received 31 January 2008; received in revised form 4 June 2008; accepted 29 June 2008

Available online 6 August 2008

Abstract

This study aimed to investigate the atrophy of the posterior cingulate cortex (PCC) and medial temporal lobe (MTL) structures (i.e., the entorhinal cortex (ERC) and hippocampus) and the regional disruption of the cingulum bundle in mild cognitive impairment (MCI) and Alzheimer's disease (AD) patients. The relationships between atrophy of these structures and regional cingulum disruption were also explored. Three-dimensional MRI and diffusion tensor imaging were applied to 19 MCI, 19 probable AD patients, and 18 normal controls (NC). Fractional anisotropy (FA) values were obtained from three different regions of the cingulum. Both MCI and AD patients showed decreased PCC volumes compared with NC. ERC atrophy was also significant in AD and MCI, while hippocampus atrophy was significant only in AD. MCI patients showed a significant FA decrease in the parahippocampal cingulum (PH-C), whereas AD patients had lower FA values in the posterior cingulate cingulum (PC-C) and PH-C, as compared with NC. However, the middle cingulate cingulum (MC-C) showed no significant FA differences between groups. Moreover, the volumes of MTL structures were significantly correlated with PH-C and PC-C FA values. In terms of PCC functional deficit in MCI or early AD, our results support both the direct effect of PCC atrophy itself and the indirect effect of cingulum fiber degeneration secondary to MTL atrophy.

© 2008 Elsevier Inc. All rights reserved.

Keywords: Posterior cingulate cortex; Entorhinal cortex; Hippocampus; Cingulum; Medial temporal lobe; Atrophy; Volume; Fractional anisotropy

1. Introduction

Although structural neuroimaging studies have consistently shown the earliest volume losses in medial temporal lobe (MTL) structures such as entorhinal cortex (ERC) and hippocampus in Alzheimer's disease (AD) and mild

cognitive impairment (MCI) (Bottino et al., 2002; Convit et al., 1997; Jack et al., 1999; Killiany et al., 2002; Mosconi et al., 2005; Pennanen et al., 2004; Xu et al., 2000), functional imaging studies have revealed that hypometabolism or hypoperfusion first occur in the posterior cingulate cortex (PCC) in AD or MCI (Chételat et al., 2003; Ishii et al., 2003; Minoshima et al., 1997; Nestor et al., 2003a,b, 2006). This functional–structural discrepancy concerning the first brain regions involved in AD process has been hypothetically explained by PCC hypofunction due to the indirect effect of the degeneration of cingulum fibers secondary to MTL

* Corresponding author at: Department of Neuropsychiatry, Seoul National University Hospital, 28 Yongon-dong, Chongno-gu, Seoul 110-744, Republic of Korea. Tel.: +82 2 2072 2205; fax: +82 2 744 7241.

E-mail address: selfpsy@snu.ac.kr (D.Y. Lee).

atrophy, because the cingulum connects the MTL with the PCC (Wakana et al., 2004; Catani et al., 2002). Alternatively, PCC hypofunction could be due to the direct effect of early PCC atrophy.

In terms of PCC atrophy, no study has been performed yet in MCI, although two studies found that PCC volume is significantly reduced in clinically evident AD patients (Callen et al., 2001; Jones et al., 2006). In terms of cingulum bundle degeneration, several diffusion tensor imaging (DTI) studies (Fellgiebel et al., 2005; Firkbank et al., 2007; Rose et al., 2006; Takahashi et al., 2002; Xie et al., 2005; Zhang et al., 2007) have reported bundle disruption in MCI and AD. However, the majority of previous DTI studies has focused on the cingulum adjacent to the PCC or on the overall integrity of the cingulum, and thus, information concerning regional disruption patterns along the cingulum bundle in AD or MCI patients is very limited. Furthermore, the structural relationships between cingulum regional impairment and atrophy of the ERC, hippocampus, and PCC have not been clarified, although some have suggested that the hippocampus or global brain atrophy affect cingulum integrity in AD (Takahashi et al., 2002; Xie et al., 2005). In addition to MTL atrophy, PCC atrophy may also contribute to cingulum disruption in AD, because the cingulum contains efferent fibers from PCC, as well as from MTL structures.

The authors first aimed to investigate the volumetric changes of the PCC, ERC and hippocampus, and then to examine regional disruption of the cingulum bundle in patients with MCI and AD patients. In addition, we explored specific relationships between ERC, hippocampus or PCC volumetric changes and regional disruptions of the cingulum bundle, and association between brain structural changes and episodic memory performance was also evaluated.

2. Methods

2.1. Subjects

19 individuals with MCI and 19 patients with AD were recruited from a cohort regularly followed at the Dementia & Age-Associated Cognitive Decline Clinic at Seoul National University Hospital. Individuals with MCI met Peterson's criteria for amnesic MCI (Petersen, 2004): (a) memory complaint corroborated by an informant, (b) objective memory impairment for age, education and gender, (c) essentially preserved general cognitive function, (d) largely intact functional activities, (e) not demented. All MCI individuals had an overall Clinical Dementia Rating (CDR) rating (Morris, 1993) of 0.5. In terms of criterion (b), a performance score for at least one of the four episodic memory tests included in the Korean version of the Consortium to Establish a Registry for Alzheimer's disease (CERAD) neuropsychological battery (namely Word List Memory (WLM), Word List Recall (WLR), Word List Recognition (WLRc) and Constructional Recall (CR) test) (Lee et al., 2002), was below 1.5 S.D. below

the respective age-, education- and gender-specific normative mean (Lee et al., 2004). AD patients met both the Diagnostic and Statistical Manual of Mental Disorders (DSM-IV) criteria for dementia (American Psychiatric Association, 1994) and the National Institute of Neurological and Communication Disorders and Stroke/Alzheimer's Disease and Related Disorders Association (NINCDS-ADRDA) criteria for probable AD (Mckhann et al., 1984). 18 healthy normal controls with an overall CDR of 0 were also selected from a pool of volunteers. All subjects were included after a standardized clinical assessment and neuropsychological testing, as described below.

The following exclusion criteria were applied to all subjects: any present serious medical, psychiatric, or neurological disorder that could affect mental function; evidence of focal brain lesions on MRI including lacunes and white matter hyperintensity lesions of grade 2 or more by Fazekas scale (Fazekas et al., 1987); the presence of severe behavioral or communication problems that would make a clinical or MRI examination difficult; ambidextrousness or left-handedness; and the absence of a reliable informant.

The Institutional Review Board of Seoul National University Hospital, approved the study protocol and informed consent was obtained from all study subjects and their relatives.

2.2. Clinical and neuropsychological assessments

All subjects were examined by neuropsychiatrists with advanced training in neuropsychiatry and dementia research according to the protocol of the Korean Version of the CERAD Assessment Packet (Lee et al., 2002). Psychiatric, general physical and neurological examinations; routine laboratory tests; MRI of the brain; the CERAD neuropsychological battery, including Verbal fluency, 15-item Boston naming test; Mini-Mental State Examination (MMSE), WLM, WLR, WLRc, Constructional praxis, and CR, was also applied by experienced clinical psychologists. A panel consisting of four neuropsychiatrists with expertise in dementia research made clinical decisions, including the assignment of CDR rating. All clinical assessments were carried out within 4 weeks of MRI examination.

2.3. MRI acquisition

MRI was performed using a 3.0-T GE whole body imaging system (GE VH/I; General Electric, Milwaukee, WI, USA). A dual spin-echo echo-planar imaging (EPI) sequence was used to acquire DTI images. MR images with 25 non-collinear diffusion gradients and without diffusion gradient were acquired (TR = 10000 ms, TE = 77.1 ms, B-factor = 1000 s/mm², matrix = 128 × 128, slice thickness/gap = 3.5/0 mm, FOV = 240 mm, slice number = 38). A three-dimensional T1-weighted spoiled gradient recalled echo (SPGR) sequence was obtained for volumetric tracing and anatomical localization (TR = 22.0 ms, TE = 4.0 ms, slice thick-

ness/gap = 1.4/0 mm, matrix = 256×192 , FOV = 240 mm, Flip angle = 40°). Additionally, fluid-attenuated inversion recovery (FLAIR) and T2-weighted images were also obtained for qualitative clinical reading.

2.4. Volumetric measurement

The anatomical boundaries of ERC, hippocampus and PCC were traced manually on T1-weighted images using Analyze AVW 5.0 (Biomedical Imaging Resource, Mayo Foundation, Rochester, MN) by one of the authors (I.H.C.), who was blind to diagnosis, sex, or subject demographics. Sagittal SPGR sequence Images were realigned to a standard orientation and reformatted using sinc interpolation to a 0.94-mm slice thickness in the axial plane. The standard alignment was based on the interhemispheric fissure, the lenses of both eyes, and the line connecting the anterior and posterior commissures in the sagittal plane.

2.4.1. ERC

ERC volumes were traced according to histology-based criteria, which were designed for MRI volumetric measurements (Insausti et al., 1998). To facilitate tracing consistency, anterior/posterior boundaries were modified as follows. The anterior boundary of the ERC was 2 mm posterior to the fronto-temporal junction and its posterior boundary was 2 mm posterior to the gyrus intralimbicus. The superomedial boundary of the ERC in rostral sections was the sulcus semiannularis which separates the gyrus ambiens from amygdala and in caudal sections was the inferior border of the subiculum. The inferolateral boundary of the ERC was the lateral branch of the collateral sulcus or the rhinal sulcus. Only one of these two was usually present on a particular section. If both sulci and the two parts of the interrupted collateral sulcus were present on the same section, the one most medially located was used as the inferolateral border of the ERC.

2.4.2. Hippocampus

Tracing began with the generation of the auxiliary guideline traces on the sagittal plane, and included the subiculum, Ammon's horn (hippocampus proper), and the dentate gyrus (Pantel et al., 2000). And the regions of interest were finally defined on the coronal plane. The borders of the hippocampus were defined as follows. For the hippocampal head, medial/lateral borders are the ambient gyrus or entorhinal sulcus/the temporal horn of the lateral ventricle and dorsal/ventral borders are the alveous/the white matter of the temporal lobe or the subiculum. For the body of the hippocampus, medial/lateral border is the ambient cistern and the crus cerebri/the temporal stem and inferior horn of the lateral ventricle and dorsal/ventral borders are the CSF of the lateral ventricle/the white matter of the temporal lobe. For the tail of the hippocampus, medial/lateral borders are the CSF of the atrium of the lateral ventricles/the ascending crus of the fornix and dorsal/ventral borders are the pulvinar of the thalamus/the white matter of the temporal lobe.

2.4.3. PCC

The posterior cingulate cortex was marked sagittally and traced coronally using sagittal markings according to a previously described guideline (Callen et al., 2001). Posterior/anterior boundaries were from the posterior tip of the subparietal sulcus to the posterior commissure. Inferior/superior boundaries were from the callosal sulcus to the cingulate and subparietal sulci. Medial/lateral boundaries were from the longitudinal fissure to the most lateral gray matter marked sulcus.

2.4.4. Intracranial volume

Intracranial volume (ICV) was used to correct for possible differences in regional volumes resulting from preexisting differences in total brain size as indexed by skull capacity. ICV tracings were made using a previously described method (Buckner et al., 2004).

To determine the reliability of volumetric measurements, the same rater, unaware of previous readings, repeated volume tracing on 10 randomly selected subjects. Reliability, expressed as intraclass correlation coefficients, was 0.97 for the hippocampus, 0.94 for the ERC, and 0.96 for the PCC.

2.5. DTI data postprocessing

In order to better compensate for the poor interslice resolution of DTI images, the authors interpolated the image volume along with slice direction to be spatially isotropic (Oh et al., 2007). One voxel size of the resulting DTI images was $0.94 \text{ mm} \times 0.94 \text{ mm} \times 0.94 \text{ mm}$.

Fractional anisotropy (FA: a measure for white matter integrity), mean diffusivity (MD: a measure for randomized mean water diffusion) (Le Bihan et al., 2001) and color-coded directionality diffusion maps (Pajevic and Pierpaoli, 1999) were created off-line from the DTI images, using an IDL (Interactive Data Language, Research Systems Inc., Boulder, Colorado, USA) 6.0-based in-house program. In order to place the volumes of interest (VOIs), FA, MD and color-coded maps were overlaid. The color-coded directional maps (red: left-to-right direction, green: anterior-to-posterior direction, blue: superior-to-inferior direction) enable white matter fiber tracts to be easily visualized. Cubic VOIs were placed based on the cingulum bundle on the color-coded maps of each subject. Three pairs (left and right) of VOIs were placed on sagittal slices to select the following regions of the cingulum bundle: bilateral parahippocampal regions (at the medial temporal portion of the cingulum fibers (PH-C)), bilateral posterior cingulate regions (at the level of the posterior dorsal curve of the cingulum fibers (PC-C)), and bilateral middle cingulate regions (at the center of the dorsal curve of the cingulum fibers (MC-C)) (Fig. 1). To obtain standardized conditions for analysis and to avoid data contamination by adjacent structures, all VOIs were fixed as $2.82 \text{ mm} \times 2.82 \text{ mm} \times 2.82 \text{ mm}$ (i.e., $3 \times 3 \times 3$ voxels). An experienced neuropsychiatrist (I.H.C.), blinded to subject information including diagnosis, placed the VOIs. FA

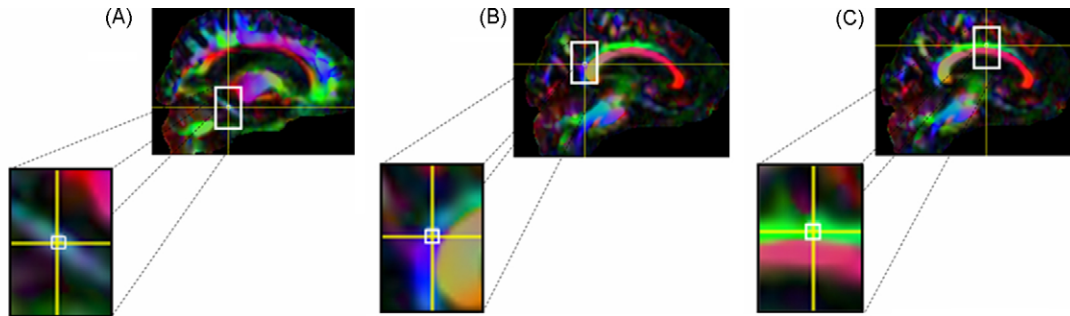


Fig. 1. Illustrations of volume of interest (VOI) selection on color-coded maps (red: left-to-right direction, green: anterior-to-posterior direction, blue: superior-to-inferior direction) for FA and MD determination: (A) VOI at the parahippocampal region of the cingulum; (B) VOI at the posterior cingulate region of the cingulum; and (C) VOI at the middle cingulate region of the cingulum.

and MD values within each VOI were averaged. To determine the reliability of VOI measurements, the same rater, unaware of previous readings, repeated VOI drawings on 10 randomly selected subjects. Intrarater reliability, expressed as a mean intraclass correlation coefficient, was 0.98 for the DTI measurements.

2.6. Statistics

The demographic and clinical data from the three groups were compared by one-way ANOVA. To compare proportions and categorical data, the χ^2 test was applied. Since analyzed DTI and volumetric data did not show substantial deviation from normal distribution, parametric tests were also used. Group differences in DTI and volumetric data were tested by one-way analyses of variance (ANOVAs) with Scheffe's post hoc tests. For these analyses, each regional volume was normalized by ICV for individual subjects using the formula (absolute regional volume in mm^3/ICV in mm^3) $\times 1000$. Relations between DTI and volumetric data, or between DTI or volumetric data and WLR or other CERAD neuropsychological test scores, were analyzed using partial correlation analyses controlling age and ICV. Cognitive test raw scores were transformed to *T*-scores, based on normative data for the healthy elderly Korean population (Lee et al., 2002). The level of statistical significance was set at two-tailed $p < 0.05$. All analyses were performed using SPSS software, version 12.0 (SPSS Inc, USA).

3. Results

3.1. Demographic characteristics

Subject characteristics are summarized in Table 1. The MCI, AD and NC groups were similar in terms of age ($p = 0.906$, by ANOVA), education ($p = 0.125$, by ANOVA) and gender ($\chi^2 = 0.236$, $p = 0.889$). AD patients had significantly lower MMSE scores than NC ($p < 0.001$) or MCI subjects ($p < 0.001$), but no significant difference was found between NC and MCI ($p = 0.064$). AD patients showed

markedly lower WLR test scores than NC ($p < 0.001$) or MCI subjects ($p = 0.008$), and MCI patients also had lower WLR scores than NC subjects ($p < 0.001$). CDR distributions within each group are also presented in Table 1.

3.2. Group comparisons of volumetric values

Mean normalized ERC, hippocampal and PCC volumes are summarized in Table 2. Both MCI and AD patients showed significantly lower normalized bilateral ERC volume than NC subjects, while there was no difference between MCI and AD patients. In terms of the normalized hippocampus volume, AD patients had significantly lower values than controls bilaterally, while MCI patients and controls were similar. AD patients also had lower left hippocampus volumes than MCI patients. Moreover, MCI and AD patients showed significantly lower normalized bilateral PCC volumes than controls, and AD patients had lower bilateral PCC volumes than MCI patients.

Table 1
Demographic and clinical characteristics of subjects

	NC ($n = 18$)	MCI ($n = 19$)	AD ($n = 19$)
Gender (M/F)	6/12	6/13	5/14
Age (year)	70.7 \pm 5.2	71.6 \pm 7.1	71.1 \pm 5.1
Education (year)	10.7 \pm 3.3	7.5 \pm 5.6	8.3 \pm 5.5
CDR			
0	18	0	0
0.5	0	19	6
1	0	0	11
2	0	0	2
MMSE	49.4 \pm 8.3	35.5 \pm 8.4	-1.8 \pm 27.8 [†]
WLR	57.5 \pm 9.6	35.1 \pm 8.1*	26.0 \pm 8.1 [†]

Values are expressed as means \pm S.D. MMSE and WLR test scores are age, education and gender-specific norm corrected *T*-scores. NC = normal controls; MCI = Mild Cognitive Impairment; AD = Alzheimer disease; CDR = clinical dementia rating; MMSE = Mini-mental state examination; WLR = Word List Recall test.

* Significantly different from NC ($p < 0.001$, by Scheffe's post hoc test).

[†] Significantly different from NC and MCI ($p < 0.001$ and $p = 0.008$, respectively, by Scheffe's post hoc test).

Table 2

Group comparisons of the normalized volumes* of the posterior cingulate cortex, entorhinal cortex and hippocampus

	NC (n = 18)	MCI (n = 19)	AD (n = 19)	p-Values [†]		
				NC vs. MCI	NC vs. AD	MCI vs. AD
ERC volume						
Right	0.69 ± 0.15	0.37 ± 0.05	0.35 ± 0.12	<0.001	<0.001	0.804
Left	0.72 ± 0.14	0.42 ± 0.07	0.37 ± 0.10	<0.001	<0.001	0.349
HIP volume						
Right	2.45 ± 0.32	2.20 ± 0.36	1.93 ± 0.33	0.088	<0.001	0.056
Left	2.29 ± 0.35	2.11 ± 0.37	1.80 ± 0.31	0.272	<0.001	0.024
PCC volume						
Right	1.41 ± 0.36	1.00 ± 0.28	0.75 ± 0.23	<0.001	<0.001	0.038
Left	1.34 ± 0.25	1.05 ± 0.32	0.76 ± 0.26	<0.001	<0.001	0.009

All values are mean ± S.D. NC = normal controls; MCI = Mild Cognitive Impairment; AD = Alzheimer disease; ERC = entorhinal cortex; HIP = hippocampus; PCC = posterior cingulate cortex.

* Normalized volume = (regional volume × 10³)/(total intracranial volume).

† Scheffe's post hoc test.

3.3. Group DTI comparisons

Mean FA values are given in Table 3. MCI patients had significantly lower left PH-C FA values than controls, and AD patients had lower bilateral PH-C and left PC-C FA values than controls. AD and MCI patients had similar bilateral PH-C and PC-C FA values. MC-C FA values were similar in the three groups. MD values of the three cingulum regions were similar in all three groups.

3.4. Correlations between volumetric and DTI values

We first performed partial correlation analyses controlling age and ICV for the data combined across the three groups (n = 56). In the left hemisphere, ERC and hippocampus volumes were significantly correlated with PH-C and PC-C FA (ERC vs. PH-C: $r = 0.508$, $p < 0.001$; ERC vs. PC-C: $r = 0.414$, $p = 0.002$; hippocampus vs. PH-C: $r = 0.365$, $p = 0.007$; and hippocampus vs. PC-C: $r = 0.443$, $p < 0.001$). In the right hemisphere, ERC volume was found to be significantly correlated with PH-C ($r = 0.513$, $p < 0.001$) and PC-C FA ($r = 0.357$, $p = 0.008$), while hippocampus volume

was significantly correlated only with PC-C FA ($r = 0.455$, $p < 0.001$), but not with PH-C FA. For both hemispheres, the volumes of the two MTL structures were not correlated with MC-C FA values. In addition, PCC volume was not significantly correlated with any regional cingulum FA values.

Very similar results were found from the partial correlation analyses for the data combined across MCI and AD (n = 38). In the left hemisphere, ERC volume was significantly correlated with PH-C ($r = 0.490$, $p = 0.002$) and PC-C FA ($r = 0.412$, $p = 0.013$), while hippocampus volume was not correlated with the FA values of those two regions. In the right hemisphere, ERC volume was significantly correlated with PH-C ($r = 0.374$, $p = 0.025$) and PC-C ($r = 0.368$, $p = 0.027$). Hippocampus volume was not correlated with PH-C FA, but with PC-C FA ($r = 0.459$, $p = 0.005$). For both hemispheres, no significant correlations were found between any regional volume and MC-C, or between PCC volume and any regional FA value.

In contrast, within NC group, no significant correlations were observed between any regional volume and any regional FA value of the cingulum.

Table 3

Group comparisons of the regional fractional anisotropy (FA) values of the cingulum bundle

	NC (n = 18)	MCI (n = 19)	AD (n = 19)	p-Values*		
				NC vs. MCI	NC vs. AD	MCI vs. AD
PH-C FA						
Right	0.35 ± 0.06	0.30 ± 0.05	0.29 ± 0.08	0.078	0.028	1.000
Left	0.37 ± 0.05	0.32 ± 0.06	0.30 ± 0.06	0.024	0.001	0.565
PC-C FA						
Right	0.35 ± 0.05	0.32 ± 0.05	0.30 ± 0.08	0.482	0.081	0.554
Left	0.34 ± 0.05	0.32 ± 0.04	0.29 ± 0.06	0.548	0.048	0.355
MC-C FA						
Right	0.38 ± 0.08	0.34 ± 0.05	0.36 ± 0.06	0.209	0.762	0.566
Left	0.37 ± 0.06	0.36 ± 0.07	0.34 ± 0.06	0.966	0.462	0.606

All values are mean ± S.D. NC = normal controls; MCI = Mild Cognitive Impairment; AD = Alzheimer disease; PH-C = parahippocampal cingulum; PC-C = posterior cingulate cingulum; MC-C = middle cingulate cingulum.

* Scheffe's post hoc test.

3.5. Correlations between neuropsychological test scores and volumetric or FA values

Partial correlation analyses were conducted between WLR or any other CERAD neuropsychological test scores and regional volumetric or FA values, controlling age and ICV, for the data combined across the three groups ($n=56$). WLR scores were found to be significantly correlated with bilateral ERC, hippocampus, and PCC volumes (left ERC: $r=0.861$; right ERC: $r=0.843$; left hippocampus: $r=0.558$; right hippocampus: $r=0.591$; left PCC: $r=0.608$; and right PCC: $r=0.636$, $p<0.001$ for all correlations), and with bilateral PH-C and PC-C FA values (left PH-C: $r=0.418$, $p=0.002$; right PH-C: $r=0.332$, $p=0.014$; left PC-C: $r=0.332$, $p=0.014$; and right PC-C: $r=0.338$, $p=0.012$). In contrast, bilateral MC-C FA values were not found to be significantly correlated with WLR scores. Correlations between other CERAD neuropsychological test scores and volume or FA values are presented in [Supplementary Table](#).

4. Discussion

Our findings of significantly reduced ERC and hippocampus volumes in AD patients versus normal controls are comparable, in general, to those of previous volumetric studies ([Bottino et al., 2002](#); [Convit et al., 1997](#); [Du et al., 2001](#); [Killiany et al., 2002](#); [Pennanen et al., 2004](#); [Xu et al., 2000](#)). In addition, we also found a significant ERC volume reduction in MCI patients versus controls and a significant hippocampus volume reduction in AD patients versus MCI patients. These findings suggest that ERC volume loss precedes hippocampus volume loss during early AD development, assuming that MCI represent a preclinical stage of AD. Our results agree well with published pathological evidence indicating that the earliest neuropathological changes in AD occur in the ERC and then progress to the hippocampus and other limbic structures ([Braak and Braak, 1991](#); [Braak et al., 1993](#)). One previous study concluded that ERC volume loss dominates hippocampus volume loss in MCI, but that in mild AD hippocampal volume loss is more pronounced ([Pennanen et al., 2004](#)). Our results also confirmed the findings of two earlier volumetric studies ([Callen et al., 2001](#); [Jones et al., 2006](#)) which showed that PCC volumes are significantly reduced in AD. This finding is in-line with voxel-based morphometric data, which revealed reduced grey matter density ([Baron et al., 2001](#); [Frisoni et al., 2002](#)), and with pathological data showing neuronal degeneration ([Vogt et al., 1990, 1998](#)) in the PCCs of AD patients. Moreover, we first found that PCC volume loss is significant even in MCI. Comparable to this result, a recent in vivo molecular imaging study ([Small et al., 2006](#)) showed that marked AD-related neuropathological changes are present in the PCC and in medial temporal structures in MCI patients.

In terms of cingulum bundle disruption, our results show that FA reductions are most prominent in the parahippocam-

pal region in MCI, and the cingulum fibers near the posterior cingulate and parahippocampal region are associated with FA reductions in AD. In contrast, the cingulum region adjacent to the middle cingulate gyrus showed no FA reduction in MCI or AD patients. These findings suggest that cingulum fiber disruption begins near medial temporal structures and then progresses to the PC-C with AD progression from the preclinical to the clinically evident stage, and that the MC-C is preserved, at least in early AD. Several studies have reported decreased cingulum bundle anisotropy in AD and MCI ([Fellgiebel et al., 2005](#); [Firbank et al., 2007](#); [Rose et al., 2006](#); [Takahashi et al., 2002](#); [Xie et al., 2005](#); [Zhang et al., 2007](#)), but the majority addressed only the PC-C and not regional disruption patterns of the cingulum bundle. Nevertheless, a recent DTI study ([Zhang et al., 2007](#)) investigated PH-C and PC-C in this context, and reported FA reductions at both cingulum regions in AD and MCI. However, other cingulum regions were not examined and the overall patterns of cingulum degeneration during early stage AD were not clearly determined. In contrast to our results, another study reported FA reduction of the MC-C in AD ([Takahashi et al., 2002](#)). This discrepancy probably results from the difference in disease severity of study subjects. Six of ten AD subjects included in the study were at a moderately severe stage, whereas 17 of 19 AD patients in our study had very mild or mild forms of the disease.

PC-C FA, as well as PH-C FA, was found to be positively correlated with the volumes of MTL structures, especially the ERC. Considering this finding with the results of our FA and volume group comparisons, it suggests that the anterograde Wallerian degeneration of the axonal fibers originated from the MTL probably contribute to cingulum disruption. This may explain the functional–structural discrepancy concerning the first brain regions, although other kinds of changes independent of AD grey matter pathology, such as loss of myelin or oligodendrial cells, also occur in AD white matter ([Brun and Englund, 1986](#)). Then, within MTL, HC did not show correlation with PH-C or PC-C disruption as consistently as ERC did. This appears to correspond with the findings from non-human primate studies ([Mufson and Pandya, 1984](#); [Amaral et al., 1984](#)), which indicate that HC is not directly interconnected to the cingulum while ERC is. One previous study reported a positive correlation between hippocampus volumes and the average FA values of whole cingulum bundle ([Xie et al., 2005](#)). However, they did not examine region-specific relations between cingulum FA values and the volumes of nearby cortical structures.

PC-C disruption did not show significant correlation with PCC volume, although PCC atrophy was also found in MCI and early AD patients. When compared to the influence of MTL atrophy, this differential contribution of PCC atrophy to cingulum disruption could be, in part, explained by cingulum anatomy. The PC-C contains long fibers, which originate from the MTL and run bypassing the PCC, as well as shorter fibers, which interconnect the MTL and the PCC ([Catani et al., 2002](#)). For this reason, MTL atrophy appears to influence

PC-C disruption to a greater extent than PCC atrophy, despite of its topographical distance from the PC-C.

The associations of the anisotropic changes of the cingulum or volumetric reductions in the ERC, hippocampus or PCC with delayed verbal recall scores support the clinical validity of our findings and generally coincide with the findings of previous studies regarding the importance of these structures in episodic memory function (Fellgiebel et al., 2005; Kalus et al., 2006; Müller et al., 2005; Nestor et al., 2006).

Summarizing, our findings indicate that cingulum disruption, adjacent to the parahippocampal gyrus and PCC, is more associated with MTL atrophy than PCC atrophy in MCI and AD, although PCC volume itself is significantly decreased even in MCI as well as in AD. Concerning PCC metabolic or perfusion deficits in MCI or early AD, our results support the possibility of both direct and indirect effect by two structural brain changes, namely the direct effect of PCC atrophy itself and the indirect effect of cingulum fiber degeneration secondary to MTL atrophy. Moreover, additive or synergistic interactions between these two structural changes may possibly explain the prominent functional PCC abnormalities observed in MCI and early AD.

Disclosure

We have no conflicts of interest to disclose. We have no contracts relating to our research with any organization that could benefit financially from our research. There are no agreements that involve any financial interest in our work.

Acknowledgement

This study was supported by the Seoul National University Hospital Research Fund (Grant No. 04 - 2006 - 091).

Appendix A. Supplementary data

Supplementary data associated with this article can be found, in the online version, at doi:10.1016/j.neurobiolaging.2008.06.015.

References

- Amaral, D.G., Insausti, R., Cowan, W.M., 1984. The commissural connections of the monkey hippocampal formation. *J. Comp. Neurol.* 224 (3), 307–336.
- American Psychiatric Association, 1994. *Diagnostic and Statistical Manual of Mental Disorders*, 4th ed. Washington, DC.
- Baron, J.C., Chételat, G., Desgranges, B., Perchev, G., Landeau, B., de la Sayette, V., Eustache, F., 2001. In vivo mapping of gray matter loss with voxel-based morphometry in mild Alzheimer's disease. *Neuroimage* 14 (2), 298–309.
- Bottino, C.M., Castro, C.C., Gomes, R.L., Buchpiguel, C.A., Marchetti, R.L., Neto, M.R., 2002. Volumetric MRI measurements can differentiate Alzheimer's disease, mild cognitive impairment, and normal aging. *Int. Psychogeriatr.* 14 (1), 59–72.
- Braak, H., Braak, E., 1991. Neuropathological staging of Alzheimer-related changes. *Acta Neuropathol.* 82 (4), 239–259.
- Braak, H., Braak, E., Bohl, J., 1993. Staging of Alzheimer-related cortical destruction. *Eur. Neurol.* 33 (6), 403–408.
- Brun, A., Englund, E., 1986. A white matter disorder in dementia of the Alzheimer's type: a pathoanatomical study. *Ann. Neurol.* 19 (3), 253–262.
- Buckner, R.L., Head, D., Parker, J., Fotenos, A.F., Marcus, D., Morris, J.C., Snyder, A.Z., 2004. A unified approach for morphometric and functional data analysis in young, old, and demented adults using automated atlas-based head size normalization: reliability and validation against manual measurement of total intracranial volume. *Neuroimage* 23 (2), 724–738.
- Callen, D.J., Black, S.E., Gao, F., Caldwell, C.B., Szalai, J.P., 2001. Beyond the hippocampus: MRI volumetry confirms widespread limbic atrophy in AD. *Neurology* 57 (9), 1669–1674.
- Catani, M., Howard, R.J., Pajevic, S., Jones, D.K., 2002. Virtual in vivo interactive dissection of white matter fasciculi in the human brain. *NeuroImage* 17 (1), 77–94.
- Chételat, G., Desgranges, B., de la Sayette, V., Viader, F., Eustache, F., Baron, J.C., 2003. Mild cognitive impairment: Can FDG-PET predict who is to rapidly convert to Alzheimer's disease? *Neurology* 60 (8), 1374–1377.
- Convit, A., De Leon, M.J., Tarshish, C., De Santi, S., Tsui, W., Rusinek, H., George, A., 1997. Specific hippocampal volume reductions in individuals at risk for Alzheimer's disease. *Neurobiol. Aging* 18 (2), 131–138.
- Du, A.T., Schuff, N., Amend, D., Laakso, M.P., Hsu, Y.Y., Jagust, W.J., Yaffe, K., Kramer, J.H., Reed, B., Norman, D., Chui, H.C., Weiner, M.W., 2001. Magnetic resonance imaging of the entorhinal cortex and hippocampus in mild cognitive impairment and Alzheimer's disease. *J. Neurol. Neurosurg. Psychiatry* 71 (4), 441–447.
- Fazekas, F., Chawluk, J.B., Alavi, A., Hurtig, H.I., Zimmerman, R.A., 1987. MR signal abnormalities at 1.5T in Alzheimer's dementia and normal aging. *Am. J. Radiol.* 149 (2), 351–356.
- Fellgiebel, A., Müller, M.J., Wille, P., Dellani, P.R., Scheurich, A., Schmidt, L.G., Stoeter, P., 2005. Color-coded diffusion-tensor-imaging of posterior cingulate fiber tracts in mild cognitive impairment. *Neurobiol. Aging* 26 (8), 1193–1198.
- Firbank, M.J., Blamire, A.M., Krishnan, M.S., Teodorczuk, A., English, P., Gholkar, A., Harrison, R., O'Brien, J.T., 2007. Atrophy is associated with posterior cingulate white matter disruption in dementia with Lewy bodies and Alzheimer's disease. *NeuroImage* 36 (1), 1–7.
- Frisoni, G.B., Testa, C., Zorzan, A., Sabattoli, F., Beltramello, A., Soininen, H., Laakso, M.P., 2002. Detection of grey matter loss in mild Alzheimer's disease with voxel based morphometry. *J. Neurol. Neurosurg. Psychiatry* 73 (6), 657–664.
- Insausti, R., Juottonen, K., Soininen, H., Insausti, A.M., Partanen, K., Vainio, P., Laakso, M.P., Pitkänen, A., 1998. MR volumetric analysis of the human entorhinal, perirhinal, and temporopolar cortices. *Am. J. Neuro-radiol.* 19 (4), 659–671.
- Ishii, K., Mori, T., Hirano, N., Mori, E., 2003. Glucose metabolic dysfunction in subjects with a clinical dementia rating of 0.5. *J. Neurol. Sci.* 215 (1–2), 71–74.
- Jack, C.R., Petersen, R.C., Xu, Y.C., O'Brien, P.C., Smith, G.E., Ivnik, R.J., Boeve, B.F., Waring, S.C., Tangalos, E.G., Kokmen, E., 1999. Prediction of AD with MRI-based hippocampal volume in mild cognitive impairment. *Neurology* 52 (7), 1397–1403.
- Jones, B.F., Barnes, J., Uylings, H.B.M., Fox, N.C., Frost, C., Witter, M.P., Scheltens, P., 2006. Differential regional atrophy of the cingulated gyrus in Alzheimer disease: a volumetric MRI study. *Cereb. Cortex* 16 (12), 1701–1708.
- Kalus, P., Slotboom, J., Gallinat, J., Mahlberg, R., Cattapan-Ludewig, K., Wiest, R., Nyffeler, T., Buri, C., Federspiel, A., Kunz, D., Schroth, G., Kiefer, C., 2006. Examining the gateway to the limbic system with dif-

- fusion tensor imaging: the perforant pathway in dementia. *NeuroImage* 30 (3), 713–720.
- Killiany, R.J., Hyman, B.T., Gomez-Isla, T., Moss, M.B., Kikinis, R., Jolesz, F., Tanzi, R., Jones, K., Albert, M.S., 2002. MRI measures of entorhinal cortex vs hippocampus in preclinical AD. *Neurology* 58 (8), 1188–1196.
- Le Bihan, D., Mangin, J.F., Poupon, C., Clark, C.A., Pappata, S., Molko, N., Chabriat, H., 2001. Diffusion tensor imaging: concepts and applications. *J. Magn. Reson. Imaging* 13 (4), 534–546.
- Lee, D.Y., Lee, K.U., Lee, J.H., Kim, K.W., Jhoo, J.H., Kim, S.Y., Youn, J.C., Woo, S.I., Ha, J., Woo, J.I., 2004. A normative study of the CERAD neuropsychological assessment battery in the Korean elderly. *J. Int. Neuropsychol. Soc.* 10 (1), 72–81.
- Lee, J.H., Lee, K.U., Lee, D.Y., Kim, K.W., Jhoo, J.H., Kim, J.H., Lee, K.H., Kim, S.Y., Han, S.H., Woo, J.I., 2002. Development of the Korean version of the Consortium to Establish a Registry for Alzheimer's Disease Assessment Packet (CERAD-K): clinical and neuropsychological assessment battery. *J. Gerontol. Psychol. Sci.* 57 (1), 47–53.
- Mckhann, G., Drachman, D., Folstein, M., Katzman, R., Price, D., Stadlan, E.M., 1984. Clinical diagnosis of Alzheimer's disease: report of the NINCDS-ADRDA work group under the auspices of Department of Health and Human Services Task force on Alzheimer's disease. *Neurology* 34 (7), 939–944.
- Minoshima, S., Giordani, B., Berent, S., Frey, K.A., Foster, N.L., Kuhl, D.E., 1997. Metabolic reduction in the posterior cingulate cortex in very early Alzheimer's disease. *Ann. Neurol.* 42 (1), 85–94.
- Morris, J.C., 1993. The Clinical Dementia Rating (CDR): current version and scoring rules. *Neurology* 43 (11), 2412–2414.
- Mosconi, L., Tsui, W.H., De Santi, S., Li, J., Rusinek, H., Convit, A., Li, Y., Boppana, M., de Leon, M.J., 2005. Reduced hippocampal metabolism in MCI and AD: automated FDG-PET image analysis. *Neurology* 64 (11), 1860–1867.
- Mufson, E.J., Pandya, D.N., 1984. Some observations on the course and composition of the cingulum bundle in the rhesus monkey. *J. Comp. Neurol.* 225 (1), 31–43.
- Müller, M.J., Greverus, D., Dellani, P.R., Weibrich, C., Wille, P.R., Scheurich, A., Stoeter, P., Fellgiebel, A., 2005. Functional implications of hippocampal volume and diffusivity in mild cognitive impairment. *NeuroImage* 28 (4), 1033–1042.
- Nestor, P.J., Fryer, T.D., Hodges, J.R., 2006. Declarative memory impairments in Alzheimer's disease and semantic dementia. *NeuroImage* 30 (3), 1010–1020.
- Nestor, P.J., Fryer, T.D., Ikeda, M., Hodges, J.R., 2003a. Retrosplenial cortex (BA 29/30) hypometabolism in mild cognitive impairment (prodromal Alzheimer's disease). *Eur. J. Neurosci.* 18 (9), 2663–2667.
- Nestor, P.J., Fryer, T.D., Smielewski, P., Hodges, J.R., 2003b. Limbic hypometabolism in Alzheimer's disease and mild cognitive impairment. *Ann. Neurol.* 54 (3), 343–351.
- Oh, J.S., Song, I.C., Lee, J.S., Kang, H., Park, K.S., Kang, E., Lee, D.S., 2007. Tractography-guided statistics (TGIS) in diffusion tensor imaging for the detection of gender difference of fiber integrity in the midsagittal and parasagittal corpora callosa. *NeuroImage* 36 (3), 606–616.
- Pajevic, S., Pierpaoli, C., 1999. Color schemes to represent the orientation of anisotropic tissues from diffusion tensor data: application to white matter fiber tract mapping in the human brain. *Magn. Reson. Med.* 42 (3), 526–540.
- Pantel, J., O'Leary, D.S., Cretsingier, K., Bockholt, H.J., Keefe, H., Magnotta, V.A., Anddreasen, N.C., 2000. A new method for the in vivo volumetric measurement of the human hippocampus with high neuroanatomical accuracy. *Hippocampus* 10 (6), 752–758.
- Pennanen, C., Kivipelto, M., Tuomainen, S., Hartikainen, P., Hänninen, T., Laakso, M.P., Hallikainen, M., Vanhanen, M., Nissinen, A., Helkala, E.L., Vainio, P., Vanninen, R., Partanen, K., Soininen, H., 2004. Hippocampus and entorhinal cortex in mild cognitive impairment and early AD. *Neurobiol. Aging* 25 (3), 303–310.
- Petersen, R.C., 2004. Mild cognitive impairment as a diagnostic entity. *J. Int. Med.* 256 (3), 183–194.
- Rose, S.E., McMahon, K.L., Janke, A.L., O'Dowd, B., de Zubicaray, G., Strudwick, M.W., Chalk, J.B., 2006. Diffusion indices on magnetic resonance imaging and neuropsychological performance in amnesic mild cognitive impairment. *J. Neurol. Neurosurg. Psychiatry* 77 (10), 1122–1122.
- Small, G.W., Kepe, V., Ercoli, L.M., Siddarth, P., Bookheimer, S.Y., Miller, K.J., Lavretsky, H., Burggren, A.C., Cole, G.M., Vinters, H.V., Thompson, P.M., Huang, S.C., Satyamurthy, N., Phelps, M.E., Barrio, J.R., 2006. PET of brain amyloid and tau in mild cognitive impairment. *N. Engl. J. Med.* 355 (25), 2652–2653.
- Takahashi, S., Yonezawa, H., Takahashi, J., Kudo, M., Inoue, T., Tohgi, H., 2002. Selective reduction of diffusion anisotropy in white matter of Alzheimer's disease brains measured by 3.0 Tesla magnetic resonance imaging. *Neurosci. Lett.* 332 (1), 45–48.
- Vogt, B.A., Van Hoesen, G.W., Vogt, L.J., 1990. Laminar distribution of neuron degeneration in posterior cingulate cortex in Alzheimer's disease. *Acta Neuropathol.* 80 (6), 581–589.
- Vogt, B.A., Vogt, L.J., Vrana, K.E., Gioia, L., Meadows, R.S., Challa, V.R., Hof, P.R., Van Hoesen, G.W., 1998. Multivariate analysis of laminar patterns of neurodegeneration in posterior cingulate cortex in Alzheimer's disease. *Exp. Neurol.* 153 (1), 8–22.
- Wakana, S., Jiang, H., Nagae-Poetscher, L.M., van Zijl, P.C.M., Mori, S., 2004. Fiber tract-based atlas of human white matter anatomy. *Radiology* 230 (1), 77–87.
- Xie, S., Xiao, J.X., Wang, Y.H., Wu, H.K., Gong, G.L., Jiang, X.X., 2005. Evaluation of bilateral cingulum with tractography in patients with Alzheimer's disease. *Neuroreport* 16 (12), 1275–1278.
- Xu, Y., Jack, C.R., O'Brien, P.C., Kokmen, E., Smith, G.E., Ivnik, R.J., Boeve, B.F., Tangalos, R.G., Petersen, R.C., 2000. Usefulness of MRI measures of entorhinal cortex versus hippocampus in AD. *Neurology* 54 (9), 1760–1767.
- Zhang, Y., Schuff, N., Jahng, G.H., Bayne, W., Mori, S., Schad, L., Mueller, S., Du, A.T., Kramer, J.H., Yaffe, K., Chui, H., Jagust, W.J., Miller, B.L., Weiner, M.W., 2007. Diffusion tensor imaging of cingulum fibers in mild cognitive impairment and Alzheimer disease. *Neurology* 68 (1), 13–19.